Lunisolar Secular Resonances

Jessica Pillow

Supervisor: Dr. Aaron J. Rosengren

December 15, 2017

1 Introduction

The study of the dynamics of objects in Earth's orbit has recently become very popular in light of the growing problem of space debris. Space debris consists of objects such as broken pieces of meteors, old satellites, chips of paint, etc. It has been estimated that over 500,000 pieces of debris are currently in Earth's orbit, and about 20,000 of those pieces are large enough to be actively tracked (the smallest of these pieces are the size of a softball!). Nevertheless, all pieces of space debris are causes of concern because of how fast they are traveling. The debris can travel up to 17,500 mph and can cause significant damage on impact.

In order to stop adding to this space pollution, we must become more responsible with the objects we send into orbit. We must identify stable orbits in which to send out-of-use satellites in order to reduce the number of collisions. Such stable orbits are called graveyard orbits. In [1], [2], and [3], the authors analyze the dynamics of objects in Earth's orbit in order to find potential graveyard orbits. They are particularly interested in studying the areas where Galileo (the European Union global navigation satellite system) is located.

1.1 Regions of Earth's Orbit

There are four regions of Earth's orbit:

1. **LEO** (Low Earth Orbit): This orbit spans the altitude from 0 to 2,000 km. The objects in orbit feel the effects of

    - the gravitational attraction of Earth
    - dissipation due to the atmospheric drag
    - the Earth's oblateness effect
    - the attraction of the Moon and Sun
    - solar radiation pressure

2. **MEO** (Medium Earth Orbit): This orbit spans the altitude from 2,000 to 35,786 km. The forces felt by the objects in orbit are similar to that of LEO, except there is no atmospheric drag.

3. **GEO** (Geostationary Orbit): This region is located at the altitude of 35,786 km. Geostationary objects move with an orbital period equal to the rotational period of the Earth.

4. **HEO** (High Earth Orbit): This region refers to the space region with altitude above the geosynchronous orbit.

For this project, we only consider objects in MEO. Objects in this region experience no dissipative forces, so there exists a Hamiltonian system that describes their motion.

1.2 The Classical Elements and Delaunay Variables

There are six classical elements that we make use of when studying objects in orbit [4]:

a : semi-major axis	M : mean anomaly
e : eccentricity	ω : argument of perigee
I : inclination	Ω : longitude of the ascending node

We define the conjugate coordinates of the Delaunay variables as follows:

$$\begin{array}{ll} L = \sqrt{\mu a} & l = M \\ G = L\sqrt{1-e^2} & g = \omega \\ H = G\cos I & h = \Omega \end{array}$$

2 Reduced Hamiltonian for Galileo Resonances

In [5], the reduced Hamiltonian is formulated for our problem, which is to analyze the behavior of satellites or space debris in orbit while under the influence of lunisolar secular resonances:

- A **lunar** gravity secular resonance occurs whenever there exists an integer vector $(k_1, k_2, k_3) \in \mathbb{Z}^3 \setminus \{0\}$ such that
$$k_1\dot{\omega} + k_2\dot{\Omega} + k_3\dot{\Omega}_M = 0.$$
- A **solar** gravity secular resonance occurs whenever there exists an integer vector $(k_1, k_2, k_3) \in \mathbb{Z}^3 \setminus \{0\}$ such that
$$k_1\dot{\omega} + k_2\dot{\Omega} + k_3\dot{\Omega}_S = 0.$$

In particular, we are interested in the Galileo resonances, given by the triples $n = (2, 1, 0)$, $n = (-2, 1, -1)$, and $n = (0, 2, -1)$. The extended autonomous Hamiltonian expressed in the Delaunay (G, H, g, h) and appended canonical variables (Γ, τ), where $\dot{\tau} \equiv \partial\mathcal{H}/\partial\Gamma = \dot{\Omega}_M$, has the form

$$\mathcal{H}(G, H, \Gamma, g, h, \tau; L) = \mathcal{H}^{\text{sec}}(G, H; L) + \mathcal{H}^{\text{lp}}(G, H, g, h, \tau; L) + \dot{\Omega}_M\Gamma, \tag{1}$$

where

$$\mathcal{H}^{\text{sec}}(G, H; L) = \mathcal{H}_{J_2} + \mathcal{H}_M^{\text{sec}} + \mathcal{H}_S^{\text{sec}}, \tag{2}$$

$$\mathcal{H}^{\text{lp}}(G, H, g, h, \tau; L) = \mathcal{H}_M^{\text{lp}} + \mathcal{H}_S^{\text{lp}}. \tag{3}$$

The secular perturbations due to the oblateness of the Earth is given by

$$\mathcal{H}_{J_2}(G,H;L) = \left(\frac{J_2 R^2 \mu^4}{4L^3}\right)\left(\frac{G^2-3H^2}{G^5}\right), \tag{4}$$

and the secular perturbations due to the Moon and Sun are given by

$$\mathcal{H}_M^{\text{sec}}(G,H;L) = \frac{\mu_M(1-6C^2+6C^4)(2-3\sin^2 I_M)}{32\mu^2 a_M^3(1-e_M^2)^{3/2}} L^4 \left(5-3\frac{G^2}{L^2}\right)\left(1-3\frac{H^2}{G^2}\right), \tag{5}$$

$$\mathcal{H}_S^{\text{sec}}(G,H;L) = \frac{\mu_S(2-3\sin^2 I_S)}{32\mu^2 a_S^3(1-e_S^2)^{3/2}} L^4 \left(5-3\frac{G^2}{L^2}\right)\left(1-3\frac{H^2}{G^2}\right). \tag{6}$$

Finally, the long-periodic lunisolar Hamiltonians are given by the following:

$$\begin{aligned}
&\mathcal{H}_M^{\text{lp}}(G,H,g,h,\tau;L) \\
&\quad = \frac{15\mu_M C S^{-1}(-1+3C^2-2C^4)(2-3\sin^2 I_M)}{16\mu^2 a_M^3(1-e_M^2)^{3/2}} L^4 \left(1-\frac{G^2}{L^2}\right)\sqrt{1-\frac{H^2}{G^2}}\left(1+\frac{H}{G}\right)\cos(2g+h) \\
&\qquad - \frac{15\mu_M C^2(4C^2-3)\sin I_M \cos I_M}{16\mu^2 a_M^3(1-e_M^2)^{3/2}} L^4 \left(1-\frac{G^2}{L^2}\right)\sqrt{1-\frac{H^2}{g^2}}\left(1-\frac{H}{G}\right)\cos(-2g+h-\tau) \\
&\qquad - \frac{3\mu_M C^3 S^{-1}(1-C^2)\sin I_M \cos I_M}{8\mu^2 a_M^3(1-e_M^2)^{3/2}} L^4 \left(5-3\frac{G^2}{L^2}\right)\left(1-\frac{H^2}{G^2}\right)\cos(2h-\tau),
\end{aligned} \tag{7}$$

$$\mathcal{H}_S^{\text{lp}}(G,H,g,h;L) = \frac{15\mu_S \sin I_S \cos I_S}{16\mu^2 a_S^3(1-e_S^2)^{3/2}} L^4 \left(1-\frac{G^2}{L^2}\right)\sqrt{1-\frac{H^2}{G^2}}\left(1+\frac{H}{G}\right)\cos(2g+h-\Omega_S) \tag{8}$$

For the remainder of the discussion, we focus on the $n=(2,1,0)$ apsidal resonance in isolation.

2.1 The Reduced Hamiltonian for the $n=(2,1,0)$ apsidal resonance

The action-angle variables for the $n=(2,1,0)$ apsidal resonance are

$$\begin{aligned}
\Lambda_1 &= G/2, & \sigma_1 &= 2g+h, \\
\Lambda_2 &= -G+2H, & \sigma_2 &= h/2, \\
\Lambda_3 &= \Gamma, & \sigma_3 &= \tau.
\end{aligned} \tag{9}$$

Treating this resonance in isolation, the reduced Hamiltonian becomes

$$\begin{aligned}
\mathcal{H}(\Lambda_1,\Lambda_2,\Lambda_3,\sigma_1;L) &= \mathcal{H}^{\text{sec}}(\Lambda_1,\Lambda_2;L) + \mathcal{H}^{\text{lp}}(\Lambda_1,\Lambda_2;L) + \dot{\Omega}_M\Lambda_3 & (10)\\
&= \frac{\xi(L)}{32}\left(1-3\Lambda_1^{-1}\Lambda_2 - \frac{3}{4}\Lambda_1^{-2}\Lambda_2^2\right)\Lambda_1^{-3} \\
&\quad + \frac{\psi(L)}{16}(1-4L^{-2}\Lambda_1^2)(6+\Lambda_1^{-1}\Lambda_2)\sqrt{12-4\Lambda_1^{-1}\Lambda_2-\Lambda_1^{-2}\Lambda_2^2}\cos\sigma_1 \\
&\quad + \dot{\Omega}_M\Lambda_3, & (11)
\end{aligned}$$

where

$$
\begin{aligned}
\xi(L) &= \frac{J_2 R^2 \mu^4}{4L^3}, \\
\psi(L) &= \frac{15}{16\mu^2}\left[\frac{\mu_M C S^{-1}(-1+3C^2-2C^4)(2-3s^2 I_M)}{a_M^3(1-e_M^2)^{3/2}} + \frac{\mu_S s I_S c I_S}{a_S^3(1-e_S^2)^{3/2}}\right] L^4.
\end{aligned} \tag{12}
$$

The Hamiltonian equations become

$$
\dot{\Lambda}_1 = -\frac{\partial \mathcal{H}}{\partial \sigma_1} = \frac{\psi(L)}{16}(1-4L^{-2}\Lambda_1^2)(6+\Lambda_1^{-1}\Lambda_2)\sqrt{12-4\Lambda_1^{-1}\Lambda_2-\Lambda_1^{-2}\Lambda_2^2}\sin\sigma_1 \tag{13}
$$

$$
\begin{aligned}
\dot{\sigma}_1 = \frac{\partial \mathcal{H}}{\partial \Lambda_1} &= \frac{3\xi(L)}{32}\left(-1+4\Lambda_1^{-1}\Lambda_2+\frac{5}{4}\Lambda_1^{-2}\Lambda_2^2\right)\Lambda_1^{-4} \\
&- \frac{\psi(L)}{16}\Big[(48L^{-2}\Lambda_1+\Lambda_1^{-2}\Lambda_2+4L^{-2}\Lambda_2)\sqrt{12-4\Lambda_1^{-1}\Lambda_2-\Lambda_1^{-2}\Lambda_2^2} \\
&- (1-4L^{-2}\Lambda_1^2)(6+\Lambda_1^{-1}\Lambda_2)(2\Lambda_1^{-2}\Lambda_2+\Lambda_1^{-3}\Lambda_2^2)(12-4\Lambda_1^{-1}\Lambda_2-\Lambda_1^{-2}\Lambda_2^2)^{-1/2}\Big]\cos\sigma_1.
\end{aligned} \tag{14}
$$

We can now analyze the phase portraits for different values of Λ_2 and a, the semi-major axis. The phase portraits were drawn in MATLAB by plotting the level curves of $\mathcal{H}$. Figure 1 shows the phase portrait for $\Lambda_2 = 0.06$ and $a = 15,000$. Notice the phase portrait resembles that of the equations that govern the motion of a pendulum. Looking at Figures 2 and 3, we see bifurcations occuring, as new equilibrium points are appearing.

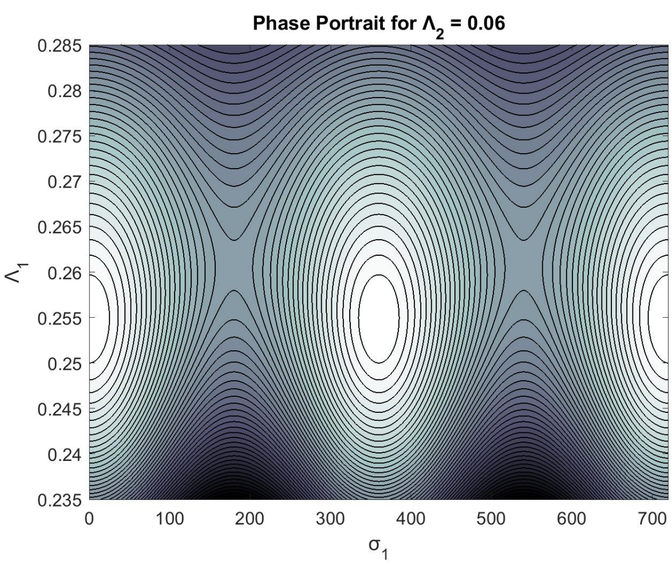

Figure 1: Phase portrait of the Hamiltonian equations for the $n = (2,1,0)$ apsidal resonance when $\Lambda_2 = 0.06$ $a = 15,000$ km.

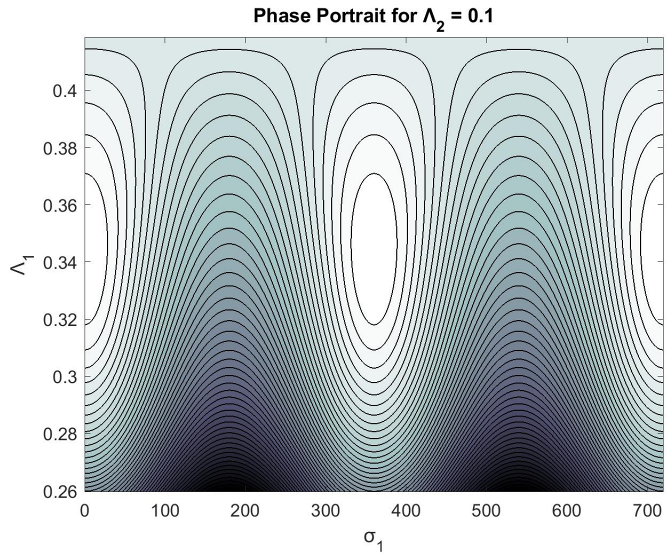

Figure 2: Phase portrait of the Hamiltonian equations for the $n = (2, 1, 0)$ apsidal resonance when $\Lambda_2 = 0.1$ and $a = 29,546$ km.

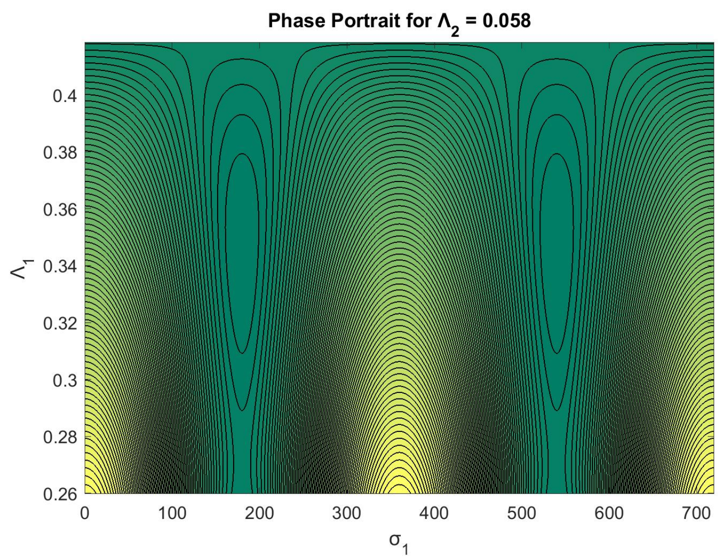

Figure 3: Phase portrait of the Hamiltonian equations for the $n = (2, 1, 0)$ apsidal resonance when $\Lambda_2 = 0.058$ and $a = 29,546$ km.

3 Conclusion

We have empirically shown that bifurcations occur in our Hamiltonian system for the $n = (2, 1, 0)$ apsidal resonance as we change the values of Λ_2 and a. Future work would entail performing rigorous bifurcation analysis on this system, as well as the systems that describe the other Galileo resonances, $n = (-2, 1, -1)$ and $n = (0, 2, -1)$. Our ultimate goal is to rigorously study the dynamics of the regions where there are overlapping resonances.

References

[1] Aaron J. Rosengren et al. Galileo disposal strategy: stability, chaos and predictability. *Monthly Notices of the Royal Astronomical Society*, 464:4063–4076, 2017.

[2] Alessandra Celletti and Catalin Gales. A study of the lunisolar secular resonance $2\dot{\omega} + \dot{\Omega} = 0$. *Frontiers in Astronomy and Space Sciences*, 3, 2016.

[3] Alessandra Celletti, Catalin Gales, and Giuseppe Pucacco. Bifurcation of lunisolar secular resonances for space debris orbits. *SIAM Journal on Applied Dynamical Systems*, 15(3):1352–1383, 2016.

[4] Harry Pollard. *Mathematical introduction to celestial mechanics*. Prentice-Hall, Inc., Englewood Cliffs, N.J., 1966.

[5] Aaron J. Rosengren. Reduced hamiltonian for lunisolar resonances. 2016.